HEAT AND MASS TRANSPORT ON A THREE-DIMENSIONAL NANOFLUID FLOW PAST A NON-LINEAR STRETCHING SHEET UNDER THE INFLUENCE OF RADIATION AND CHEMICAL REACTION

K. VERMA

Department of Mathematics, Dibrugarh University, Dibrugarh, India 786004
verma.kisu@gmail.com

***Abstract*— The main focus of the present work is to study heat and mass transfer on 3-D flow of nanofluid over a stretching sheet which is extended non-linearly in two sidewise directions. The governing equations of the problem are made dimensionless by using non-dimensional transformations and the problem is solved numerically using Matlab solver bvp4c. The temperature and concentration distributions of the fluid is determined for both linear stretching as well as non-linear stretching of the sheet for important parameters affecting the problem in graphical form and it is found that the rise in fluid temperature is always low for non-linear stretched sheet as compared to the linear one. Values of Nusselt number as well as Sherwood number are also computed to study the thermal as well as mass transfer phenomena. The numerical accuracy has also been presented by comparing the present result with existing published work.**

***Keywords*— Non-linear stretching sheet, nanofluid, radiation, heat source, chemical reaction, bvp4c**

I. INTRODUCTION

Researchers now days have been exploring the phenomenon of heat and mass transfer on different solid surface primarily due to the modern demands of various equipment's that are more efficient in dealing with the heat related issues. The focus of research interest has also been shifted to moving solid surfaces particularly because certain process like manufacturing of plastic and metal sheets, cooling of fiber etc. requires the knowledge of management of heat.

Mabood *et al.* (2015) investigated heat transmission process over a non-linear elongated surface on three-dimensional MHD nanofluid flow. Prasad *et al.* (2017) investigated nanofluid flow past a thin elastic permeable sheet sheet in a three dimensional geometry and found that the fluid velocity decreases due to suction but enhances due to injection. Mahentesh *et al.* (2017) studied numerically heat and mass transmission process of unsteady hydromagnetic nanofluid flow over an elastic elongated surface in a three dimensional system considering the important effects of Ohmic heating, thermal radiation and viscous dissipation. Kalidas *et al.* (2014) studied unsteady motion of nanofluid with the effects of thermophoresis and radiation on a hot stretched surface and found in their investigation that thermophoresis accounts for decline of heat transmission rate. Verma *et al.* (2021a) analysed thermal and mass transport process on hydromagnetic fluid flow past an extending surface in pervious medium with thermal diffusion and Dufour effects. Dhif *et al.* (2021) investigated thermal efficiency of solar collector as well as its storage capacity on hybrid nanofluid which consists of $\mathrm{Al_2O_3-SiO_2}$ as nanoparticle while $\mathrm{KNO_3-NaNO_3}$ as Phase Change Material. Verma *et al.* (2021b) investigated numerically using bvp4c numerical solver heat and mass transport process past an extending/shrinking surface in micropolar nanofluid flow with heat source, a first order chemical reaction and thermophoresis. Sadeghi *et al.* (2021) investigated nanofluid flow comprising of CuO −water in a rectangular oil water separator cavity to study its applications in power plants. Verma and Sharma (2022) investigated numerically the effects of thermal diffusion, viscous dissipation and Joule heating on MHD flow through an exponentially stretching sheet. They found in their study that consequences of Ohmic heating and viscous dissipation account for the rise in fluid temperature thereby enhancing the thermal transmission rate. Pandey and Kumar (2017a), Pandey and Kumar (2017b), Devi and Devi (2017), Maleki *et al.* (2019), Singh *et al.* (2020), Upreti *et al.* (2020), Zainal *et al.* (2021), Singh *et al.* (2021a), Upreti *et al.* (2021), Upreti *et al.* (2022), Abu-Hameda *et al.* (2021), Singh *et al* (2021b), Pandey *et al.* (2022) report other important works on nanofluid.

Over the years, the hunt for sustainable energy particularly the ones that do not harm the nature have led to several studies on solar energy. It is the best-known form of renewable energy and investigation carried out by Hunt (1978) has disclosed the fact that tiny particles can be used to collect energy emitted by sun i.e. solar energy. The work of Trieb and Nitsch (1998) disclosed the information that solar collectors based on nanofluid technology could utilize the solar energy to an optimal level. Khan *et al.* (2015) in their study discussed the influence of thermophoresis diffusion of nanoparticles accompanied by Brownian motion over a non-linear stretched surface. Considering all these aspects, we are motivated to study heat and mass transfer on nanofluid flow over a non-linear extending sheet in a three-dimensional flow. The impact of chemical reaction has been incorporated in the mass- transfer equation since it boosts the rate of mass transmission. Moreover, the impact of thermal radiation as well as external heat source are incorporated to study its influence on the nanofluid. The problem is solved numerically by Matlab inbuilt solver bvp4c.

II. MATHEMATICAL FORMULATION

Consider a flow of incompressible nanofluid produced due to non-linear stretching of a sheet in two different direction i.e. along x-axis and y-axis of the surface. The material of the sheet is assumed elastic. Let the velocities in x and y directions be u_w and v_w respectively; where $u_w = a(x+y)^m$ and $v_w = b(x+y)^m$, $a, b, m > 0$. Let the temperature at the surface of the sheet be T_w. It is also assumed that there is no mass flux at the surface of the sheet. The temperature and nanoparticles volume fraction far away from the sheet be T_∞ and C_∞ respectively. The influence of thermophoretic diffusion along with Brownian motion is consider and Buongiorno (2006) model is taken to investigate its combine effect.

The mathematical equations according to Khan *et al*. (2015) are

$$\frac{\partial u}{\partial x} + \frac{\partial v}{\partial y} + \frac{\partial w}{\partial z} = 0, \tag{1}$$

$$u\frac{\partial u}{\partial x} + v\frac{\partial u}{\partial y} + w\frac{\partial u}{\partial z} = \nu_f \frac{\partial^2 u}{\partial z^2}, \tag{2}$$

$$u\frac{\partial v}{\partial x} + v\frac{\partial v}{\partial y} + w\frac{\partial v}{\partial z} = \nu_f \frac{\partial^2 v}{\partial z^2}, \tag{3}$$

$$u\frac{\partial T}{\partial x} + v\frac{\partial T}{\partial y} + w\frac{\partial T}{\partial z} = \alpha \frac{\partial^2 T}{\partial z^2} + \tau\left[D_B \frac{\partial C}{\partial z}\frac{\partial T}{\partial z} + \frac{D_T}{T_\infty}\left(\frac{\partial T}{\partial z}\right)^2\right] - \frac{1}{\rho c_p}\frac{\partial q_r}{\partial z} + \frac{Q}{\rho c_p}(T - T_\infty), \tag{4}$$

$$u\frac{\partial C}{\partial x} + v\frac{\partial C}{\partial y} + w\frac{\partial C}{\partial z} = D_B \frac{\partial^2 C}{\partial z^2} + \frac{D_T}{T_\infty}\frac{\partial^2 T}{\partial z^2} - K_r(C - C_\infty). \tag{5}$$

The boundary conditions of the problem are

$$u = u_w = a(x+y)^m, v = v_w = b(x+y)^m,$$
$$w = 0, T = T_w, D_B\frac{\partial C}{\partial z} + \frac{D_T}{T_\infty}\frac{\partial T}{\partial z} = 0, \text{ at z=0}, \tag{6}$$

$$u \to 0, v \to 0, T \to T_\infty, C \to C_\infty \quad as\ z \to \infty. \tag{7}$$

where u, v, w symbolizes velocity components in x, y and z respectively. $\nu_f, \alpha, \tau, D_B, D_T, Q, K_r, T\ and\ C$ denotes kinematic viscosity of the fluid, thermal diffusivity, ratio of heat capacity of nanoparticles to the base fluid, Brownian diffusion coefficient, thermophoretic diffusion coefficient, heat source, rate of reaction, local fluid temperature and concentration respectively.

Heat flux due to radiation (Yih, 1999),

$$q_r = -\frac{4\sigma}{3k^*}\frac{\partial T^4}{\partial z} \tag{8}$$

Where

$$T^4 \approx 4T_\infty^3 T - 3T_\infty^4 \tag{9}$$

The following similarity transformations are used

$$u = a(x+y)^m f'(\eta), v = b(x+y)^m g'(\eta),$$
$$w = -\sqrt{a\nu_f}(x+y)^{\frac{m-1}{2}}\left(\frac{m+1}{2}(f+g) + \frac{m-1}{2}\eta(f'+g')\right),$$
$$\theta(\eta) = \frac{T - T_\infty}{T_w - T_\infty}, \phi(\eta) = \frac{C - C_\infty}{C_\infty},$$
$$\eta = \sqrt{\frac{a}{\nu_f}} z(x+y)^{\frac{m-1}{2}}. \tag{10}$$

Equation of continuity (1) is satisfied by (10) and Eqs. (2)-(5) are transformed to

$$f''' + \frac{m+1}{2}(f+g)f'' - m(f'+g')f' = 0, \tag{11}$$

$$g''' + \frac{m+1}{2}(f+g)g'' - m(f'+g')g' = 0, \tag{12}$$

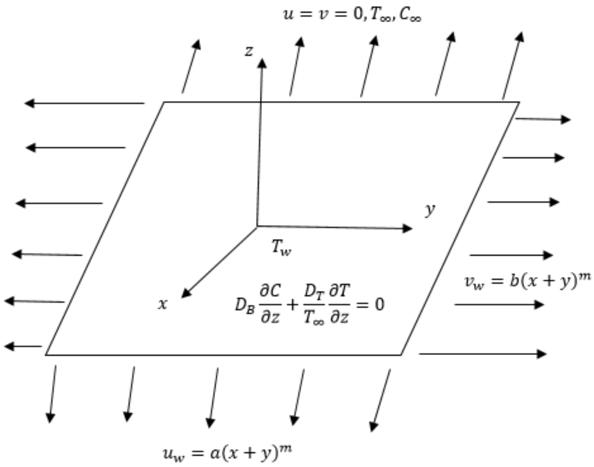

Fig. 1: Geometric model

$$\left(1 + \frac{4}{3}R_d\right)\theta'' + PrNb\phi'\theta' + PrNt\theta'^2 + Pr\delta\theta + Pr\left(\frac{m+1}{2}\right)(f+g)\theta' = 0, \tag{13}$$

$$\phi'' + \frac{Nt}{Nb}\theta'' + \left(\frac{m+1}{2}\right)(f+g)Sc\phi' - ScK_c\phi = 0. \tag{14}$$

where $\delta = \frac{Q}{(x+y)^{m-1}a\rho C_p}$, $Sc = \frac{\nu_f}{D_B}$, $Pr = \frac{\nu_f}{\alpha}$, $R_d = \frac{4\sigma T_\infty^3}{k^* k}$, $K_c = \frac{K_r}{a(x+y)^{m-1}}$, $Nt = \frac{\tau D_T(T_w - T_\infty)}{\nu_f T_\infty}$ and $Nb = \frac{\tau D_B C_\infty}{\nu_f}$ represents heat generation parameter, Schmidt number, Prandtl number, radiation parameter, chemical reaction parameter, thermophoresis parameter and Brownian motion parameter respectively.

The boundary restrictions are now transformed to

$$f(0) = g(0) = 0, f'(0) = 1, g'(0) = \lambda,$$
$$\theta(0) = 1, Nb\phi'(0) + Nt\theta'(0) = 0, \tag{15}$$

$$f'(\infty) \to 0, g'(\infty) \to 0, \theta(\infty) \to 0, \phi(\infty) \to 0. \tag{16}$$

where $\lambda = \frac{b}{a}$ is the rate of stretching.

The quantities that are important for engineering are Skin-friction coefficient, Nusselt number and Sherwood number. The are defined as follows (Khan *et al*., 2015):

Skin-friction coefficient along $x-$ direction is given by

$$C_{fx} = \frac{\tau_{zx}}{\rho_f u_w^2} = \frac{\mu\left(\frac{\partial u}{\partial z} + \frac{\partial w}{\partial x}\right)_{z=0}}{\rho_f u_w^2} = \frac{f''(0)}{Re_x^{\frac{1}{2}}},$$

or $Re_x^{\frac{1}{2}} C_{fx} = f''(0)$, where $Re_x = \frac{u_w(x+y)}{\nu_f}$ is the local Reynolds number along x −direction.

Skin-friction coefficient along $y-$ *direction* is given by

$$C_{fy} = \frac{\tau_{zy}}{\rho_f v_w^2} = \frac{\mu\left(\frac{\partial v}{\partial z} + \frac{\partial w}{\partial y}\right)_{z=0}}{\rho_f v_w^2} = \frac{g''(0)}{Re_y^{\frac{1}{2}}\lambda^{\frac{3}{2}}},$$

or $Re_y^{\frac{1}{2}}\lambda^{\frac{3}{2}} C_{fy} = g''(0)$, where $Re_y = \frac{v_w(x+y)}{\nu_f}$ is the local Reynolds number in y −direction.

Local Nusselt number is given by,

$$Nu = \frac{(x+y)q_w}{k(T_w - T_\infty)} = \frac{(x+y)\left(-k\frac{\partial T}{\partial z}\right)_{z=0}}{k(T_w - T_\infty)} = \frac{-\theta'(0)}{Re_x^{-\frac{1}{2}}},$$

or $Re_x^{-\frac{1}{2}} Nu = -\theta'(0)$.

Local Sherwood number is given by,

$$Sh = \frac{(x+y)m_w}{D_B(C_w - C_\infty)} = \frac{(x+y)\left(-D_B\frac{\partial C}{\partial z}\right)_{z=0}}{D_B(C_w - C_\infty)} = \frac{\phi'(0)}{Re_x^{-\frac{1}{2}}},$$

or $Re_x^{-\frac{1}{2}} Sh = \phi'(0)$.

III. METHOD OF SOLUTION

The solution of the present problem has been obtained numerically by solving Eqs. (11)-(14) along with boundary conditions (15) and (16) using Matlab solver bvp4c. In order to use bvp4c, Eqs. (11)-(14) are converted to first order differential equations as follows:

Let $f = y_1$, $f' = y_1' = y_2$, $f'' = y_2' = y_3$, $g = y_4$, $g' = y_4' = y_5$, $g'' = y_5' = y_6$, $,\theta = y_7$, $\theta' = y_7' = y_8$, $\phi = y_9$, $\phi' = y_9' = y_{10}$.

The first order differential equations are given by

$$y_1' = y_2, y_2' = y_3,$$

$$y_3' = -\left(\frac{m+1}{2}\right)(y_1 + y_4)y_3 + m(y_2 + y_5)y_2, y_4' = y_5,$$

$$y_5' = y_6, y_6' = -\left(\frac{m+1}{2}\right)(y_1 + y_4)y_6 + m(y_2 + y_5)y_5,$$

$$y_7' = y_8, y_8' = \frac{B}{\left(1+\frac{4}{3}Rd\right)}, y_9' = y_{10}, y_{10}' = \frac{A - \frac{Nt}{Nb}B}{\left(1+\frac{4}{3}Rd\right)},$$

where $A = -\left(\frac{m+1}{2}\right)(y_1 + y_4)\left(1 + \frac{4}{3}Rd\right)Scy_{10} + \left(1 + \frac{4}{3}Rd\right)ScK_c y_9$ and $B = -PrNby_{10}y_8 - PrNty_8^2 - Pr\delta y_7 - Pr\left(\frac{m+1}{2}\right)(y_1 + y_4)y_8$.

The boundary conditions are expressed as follows

$$y_1(0), y_4(0), y_2(0) - 1, y_5(0) - \lambda, y_7(0) - 1,$$
$$Nby_{10}(0) + Nty_8(0), y_2(\infty), y_5(\infty), y_7(\infty), y_9(\infty).$$

With the help of the bvp4c Matlab code, we obtained the solution in graphical form.

IV. RESULTS AND DISCUSSION

The numerical investigation of the present problem are done by assigning the following values of the parameters $m = 1$ (linear case), $m = 3$ (Non-linear case), $Pr = 7$, $Sc = 20$, $Nt = Nb = 0.5$, $\delta = 0.5$, $R_d = 0.1$, $K_c = 0.5$ and $\lambda = 0.5$. In addition, we have computed Nusselt number as well as Sherwood number to study heat and mass transmissions process for some important parameters involved in the problem. The parameters affecting the fluid velocity, temperature and concentration have been discussed for both linear as well non-linear stretching surface in the graphical result. Moreover, the accuracy of our study has been verified by making comparison with the work of Khan *et al.* (2015) for Nusselt number as shown in Table 1 and skin-friction coefficient along x-direction and y −direction in Table 2.

In Fig. 2, it is noticed that fluid temperature enhances with the rise in thermophoresis parameter in case of both linearly stretching sheet as well as non-linearly stretching sheet. Of course, the rise in fluid temperature is more in case of linearly stretching sheet than the non-linear ones for the same value of Nt. In Fig. 3; exponential growth on nanoparticle volume fraction up to $\eta = 0.5$ is noticed for $m = 1$ i.e. linear case after which it decreases up to the upper edge of the boundary layer. While a strict exponential growth of nanoparticles volume fraction is observed up to $\eta = 1$ for higher value of thermophoresis

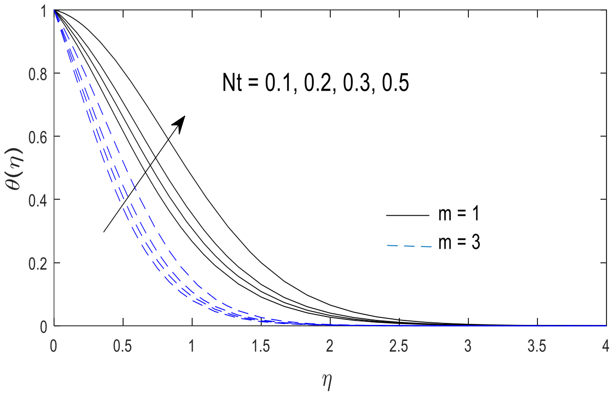

Fig. 2: Temperature distribution for Nt

Table 1: Comparison of the present result for $-\theta'(0)$ with the work of Khan et al. (2015) when $m = 3, Pr = 7, \delta = K_c = R_d = 0$.

Nt	Sc	λ	Khan *et al.* (2015)	Present work
0.1	10	0	2.4044797	2.4045
0.5			1.579305	1.5790
0.7			1.276073	1.2758
0.5	3	0.5	2.588318	2.5881
	5		2.318470	2.3183
	10		1.934245	1.9342

Table 2: Comparison of the present result for $f''(0) and\ g''(0)$ with the work of Khan et al. (2015) when $Nt = Nb = 0.5, Pr = 3, \delta = K_c = R_d = 0$.

m	λ	Khan *et al.* (2015) $f''(0)$	Present work $f''(0)$	Khan *et al.* (2015) $g''(0)$	Present work $g''(0)$
1	0	-1	-1.0014	0	0
	0.5	-1.224745	-1.2253	-0.612372	-0.6126
	1	-1.414214	-1.4144	-1.414214	-1.4144
3	0	-1.624356	-1.6245	0	0
	0.5	-1.989422	-1.9895	-0.994711	-0.9947
	1	-2.297186	-2.2972	-2.297186	-2.62972

parameter i.e. $Nt = 1$ for $m = 3$ i.e non-linear case but the peak of the growth is less than the linear case. Another observation from Fig. 3 enable us to know that nanoparticles concentration is quite more near the sheet for the linear stretching sheet in comparison to non-linear stretching sheet.

The impact of Brownian motion parameter on nanoparticle volume fraction is depicted in Fig. 4. The graphical results disclose the fact that the nanoparticle volume fraction decreases for both the cases i.e. $m = 1$ and $m = 3$ with the rise in Brownian motion parameter.

Heat generation parameter amplifies the nanofluid temperature for both cases i.e. linear and non-linear stretching sheet as noticed in Fig. 5. Just like thermophoresis parameter, in case of heat generation parameter too the increase of fluid temperature for non-linear case is less as compared to the linear one. In Fig. 6, the increase in radiation parameter hikes the nanofluid temperature drastically for linearly stretching sheet as compared to the non-linear stretched sheet. Exponential growth of fluid temperature is noticed for linearly stretching sheet up to $\eta = 1$ after which it decreases asymptotically. However, in case of non-linearly stretching sheet asymp-

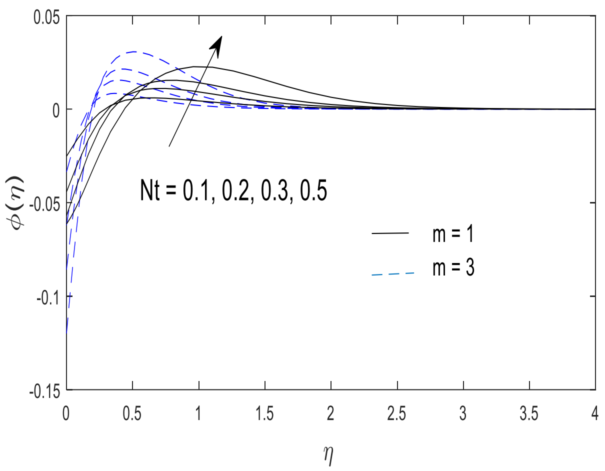

Fig. 3: Concentration distribution for Nt

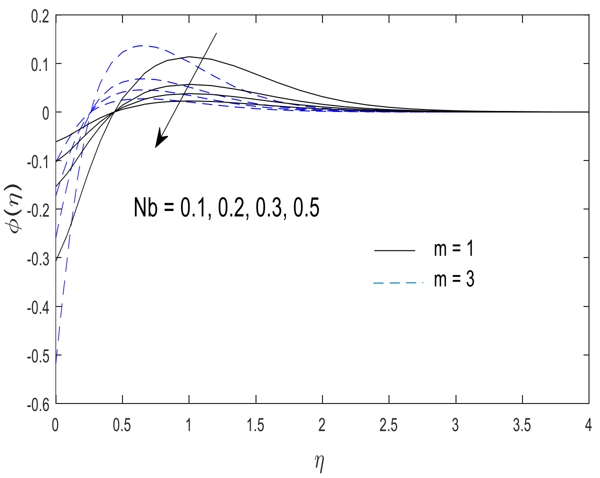

Fig. 4: Concentration distribution for Nb

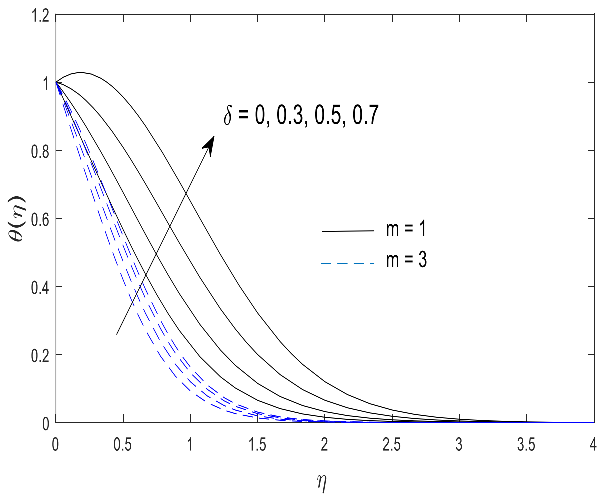

Fig. 5: Temperature distribution for δ

totic decrease of nanofluid temperature is noticed right from the surface of the sheet to the upper edge of the boundary layer.

The incorporation of chemical reaction effect is important for mass diffusion effect as it enhances the molecular diffusion activity and its result on nanoparticles

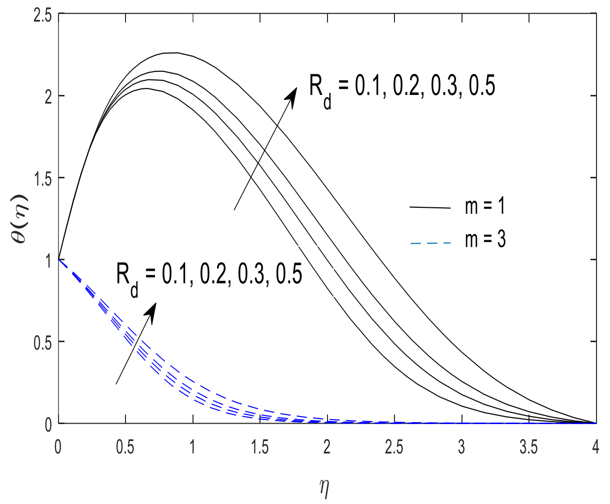

Fig. 6: Temperature distribution for R_d

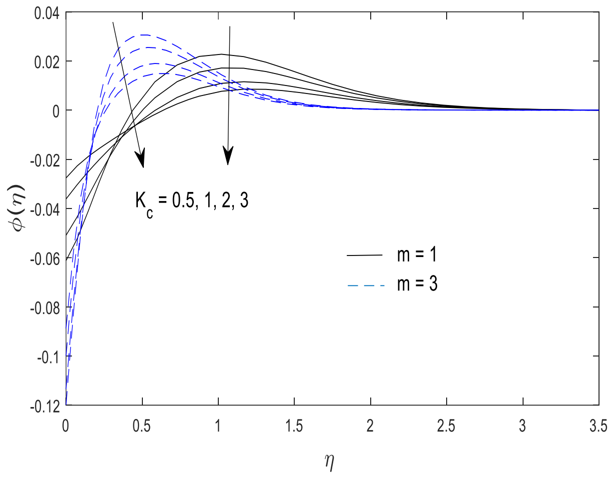

Fig. 7: Concentration distribution for K_c

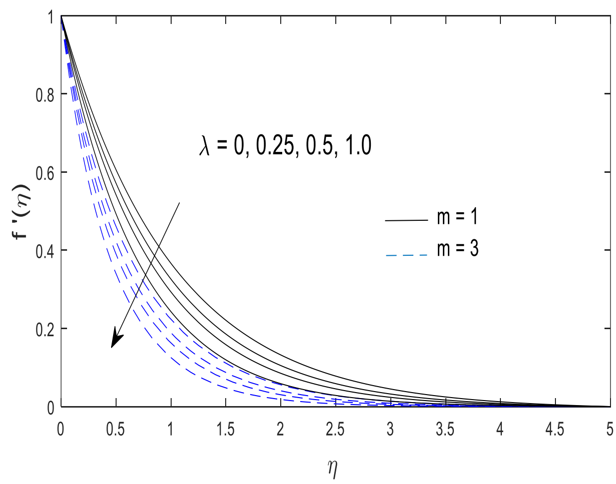

Fig. 8: Distribution of velocity component for λ along $x-$axis

volume fraction is depicted in Fig. 7. For both $m = 1$ and $m = 3$, the nanoparticle volume fraction decreases near the surface of the sheet with the increase of chemical reaction parameter due to increase in molecular diffusivity away from the sheet.

The impact of stretching ratio on $x-$ component and $y-$component of fluid velocity is shown in Fig. 8 and

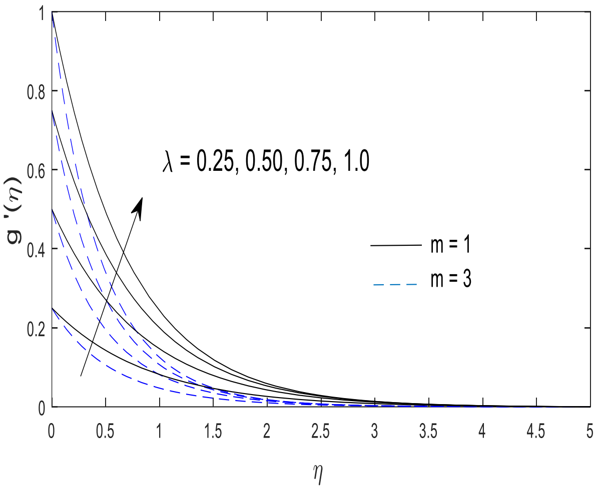

Fig. 9: Distribution of velocity component for λ along y −axis

Table 3: Numerical data for $-\theta'(0) and\ \phi'(0)$ when $m = 3$, $\mathrm{Pr} = 7$, $Nb = 0.5$, $Sc = 10$, $\lambda = 0.5$.

Nt	δ	R_d	K_c	$-\theta'(0)$	$\phi'(0)$
0.1	0.5	0.1	0.5	2.9452	0.5890
0.2				2.6644	1.0658
0.3				2.4001	1.4400
0.5					1.9341
				1.9341	
0.5	0			1.7884	1.7884
	0.3			1.3620	1.3620
	0.5			1.0259	1.0259
	0.7			0.8341	0.8351
		0.1		1.0259	1.0259
		0.2		1.0200	1.0200
		0.3		1.0094	1.0094
		0.5		0.9804	0.9804
			0.5	0.7826	0.7826
			1	0.7721	0.7721
			2	0.7534	0.7534
			3	0.7391	0.7391

Fig. 9. The figure informs that the nanofluid velocity declines with the rise in stretching ratio in the x −direction for both linear as well as non-linear case. The decrease in case of non-linearly stretching sheet is more in comparison to linearly stretching sheet. An opposite result is observed in Fig. 9 as velocity increases with the rise in stretching ratio for both linear and non-linear case.

V. CONCLUSIONS

In the present work, 3D nanofluid flow past a non-linear stretching sheet has been investigated numerically under the influence of radiation, heat source and chemical reaction. The important outcomes drawn from the above research are:

(i) Thermophoresis parameter, heat generation parameter and radiation parameter amplifies the fluid temperature for non-linear stretching sheet but the increase in temperature is always less than the linear stretched sheet.

(ii) The increase in thermophoresis parameter results in hike of nanoparticle volume fraction while it declines with the rise in Brownian motion parameter as well as chemical reaction parameter.

(iii) Fluid velocity falls with the rise in stretching ratio along x −axis but increases along y −axis.

(iv) The rate of heat transfer decreases with the rise in the values of thermophoresis parameter, heat generation parameter, chemical reaction parameter and radiation parameter. On the other hand, thermophoresis parameter accounts for the increase in mass transfer while radiation parameter, heat generation parameter and chemical reaction parameter causes it decline.

ACKNOWLEDGEMENT

I am extremely thankful to the reviewers for their important suggestions that has helped to improve the quality of the work.

ABBREVIATIONS

3D: Three-dimension

MHD: Magnetohydrodynamics

REFERENCES

Abu-Hameda, N., Alsulami, R. A., Aljinaidi, A.A., Alazwari, M.A., Eltaher, M.A., Almitani, K.H., Alnefaie, K.A., Rawa, M.J.H., Abusorrah, M.A., Sindi, H.F., Salilih, E.M. and Abulkhair, H.A. (2021) Numerical investigation of molten salt/SiO_2 nanofluid in the solar power plant cycle and examining different arrangements of shell and tube heat exchangers and plate exchangers in these cycles. *J. Taiwan Inst. of Chemical Engineers.* **124**, 1-8.

Buongiorno, J. (2006) Convective transport in nanofluids. *ASME J. Heat Transf*. **128**, 240–250.

Devi, S.U. and Devi, S.P.A. (2017) Heat transfer enhancement of $\mathrm{Cu} - \mathrm{Al_2O_3}$ /water hybrid nanofluid flow over a stretching sheet. *J. Nigerian Math. Society*. **36**, 419-433.

Dhif, K., Mebarek-Oudina, F., Chouf, S., Vaidya, H. and Chamkha, A. J. (2021) Thermal Analysis of the Solar Collector Cum Storage System Using a Hybrid-Nanofluids. *J. Nanofluids*. **10,** 634-644.

Hunt, A. J. (1978) Small particle heat exchangers, J. Renew. Sustain. Energy. *Lawrence Berkeley Lab Report Number LBL-7841*.

Kalidas, D., Duari, P.R. and Kundu, P.K. (2014) Nanofluid flow over an unsteady stretching surface in presence of thermal radiation. *Alexandria Engineering Journal*. **53**, 737-745.

Khan, J.A., Mustafa, M., Hayat, T. and Alsaedi, A. (2015) Three-dimensional flow of nanofluid over a non-linearly stretching sheet: An application to solar energy. *Int. J. of Heat and Mass Transfer*. **86**, 158-164.

Mabood, F., Khan, W.A. and Ismail, A.I.M. (2015) MHD boundary layer flow and heat transfer of nanofluids over a nonlinear stretching sheet: A numerical study. *J. Magnetism and Magnetic Materials*. **374**, 569-576.

Mahanthesh, B., Gireesha, B.J., Gorla, R.S.R. (2017) Unsteady three-dimensional MHD flow of a nano Eyring-Powell fluid past a convectively heated stretching sheet in the presence of thermal radiation, viscous dissipation and Joule heating. *J. Assoc. Arab Universities Basic Appl. Sci.* **23**, 75–84.

Maleki, H., Alsarraf, J., Moghanizadeh, A., Hajabdollahi H. and Safaei, Md. R. (2019) Heat transfer and nanofluid flow over a porous plate with radiation and slip boundary conditions. *J. Central South University*. **26**, 1099–1115.

Prasad, K.V., Vajravelu, K., Vaidya, H. and Gordec, A.V. (2017) MHD flow and heat transfer in a nanofluid over a slender elastic sheet with variable thickness, *Results in Physics*. **7**, 1462-1474.

Pandey, A.K. and Kumar, M. (2017a) Natural convection and thermal radiation influence on nanofluid flow over a stretching cylinder in a porous medium with viscous dissipation. *Alexandria Eng. J.* **56**, 55-62.

Pandey, A. K. and Kumar, M. (2017b) Boundary layer flow and heat transfer analysis on $Cu-$water nanofluid flow over a stretching cylinder with slip. *Alexandria Eng. J*. **56**, 671-677.

Pandey, A. K., Upreti, H., Joshi, N. and Uddin, Z. (2022) Effects of natural convection on 3D MHD flow of $MoS_2 - GO/H_2O$ via porous surface due to multiple slip mechanisms. *J. Taibah Univ. Sci.* **16**, 749-762.

Sadeghi, M.S., Dogonchi, A.S., Ghodrat, M. Chamlka, A.J., Alhumade, H. and Karimi, N. (2021) Natural convection of CuO-water nanofluid in a conventional oil/water separator cavity: Application to combined-cycle power plants. *J. Taiwan Instit. Chemical Engineers*. **124**, 307-319.

Singh, K., Kumar, M. and Pandey, A. K. (2020) Melting and chemical reaction effects in stagnation point flow of micropolar fluid over a stretchable porous medium in the presence of non-uniform heat source/sink. *J. Por. Media.* **28**, 767-781.

Singh, K., Pandey, A.K. and Kumar, M. (2021a) Melting heat transfer assessment on magnetic nanofluid flow past a porous stretching cylinder. *J. Egypt. Math. Society*. **29**, 1.

Singh, K., Pandey, A.K. and Kumar, M. (2021b) Numerical solution of micropolar fluid flow via stretchable surface with chemical reaction and melting heat transfer using Keller-Box Method. *Propul. Power Research*. **10**, 194-207.

Trieb, F. and Nitsch, J. (1998) Recommendations for the market introduction of solar thermal power stations. *Renew. Energy*. **14**, 17–22.

Upreti, H., Pandey, A.K., Kumar, M. and Makinde, O.D. (2020) Ohmic heating and non-uniform heat source/sink roles on 3D Darcy-Forchheimer flow of CNTs nanofluids over a stretching sheet. *Arab. J. Sci. Eng.* **45**, 7705-7717.

Upreti, H., Pandey, A.K. and Kumar, M. (2021) Assesment of entropy generation and heat transfer in three-dimensional hybrid nanofluids flow due to convective surface and base fluids. *J. Por. Media*. **4**, 35-50.

Upreti, H., Pandey, A.K., Uddin, Z. and Kumar, M. (2022) Thermophoresis and Brownian motion effects on 3D flow of Casson nanofluid consisting microorganisms over a Riga plate using PSO: A numerical study. *Chinese J. Phy.* **78**, 234-270.

Verma, K. and Sharma, B.R. (2022) Soret and Dufour effects on MHD flow with heat and mass transfer past an exponentially stretching sheet with viscous dissipation and Joule heating. *Latin American Applied Research.* **52,** 83-88.

Verma, K., Basfor, S. and Sharma, B.R. (2021a) Analysis of radiation, chemical reaction Soret and Dufour effects near stagnation point on MHD flow through a stretching sheet. *Adv. Math.: Scientific Journal*. **10**, 855-868.

Verma, K., Buragohain, D. and Sharma, B.R. (2021b) Analysis of chemical reaction on micropolar fluid flow over a shrinking sheet near stagnation point with nanoparticles and external heat. *Int. J. Heat and Technol*. **39**, 262-268.

Yih, K.A. (1999) Radiation effect on natural convection over a vertical cylinder embedded in porous medium. *Int. Comm. Heat Mass Transfer*. **26**, 259-267.

Zainal, N.A., Nazar, R., Naganthran, K. and Pop, I. (2021) Stability analysis of MHD hybrid nanofluid flow over a stretching/shrinking sheet with quadratic velocity. *Alexandria Eng. J*. **60**, 915-926.

Received: July 24, 2022
Sent to Subject Editor: August 29, 2022
Accepted: October 14, 2022
Recommended by Subject Editor Gianfranco Caruso